New Materials, Compounds and Applications
Vol.5, No.3, 2021, pp.156-170

FINITE ELEMENT MODELLING AND EXPERIMENTAL INVESTIGATION ON MECHANICAL PROPERTIES AND MICRO STRUCTURAL STUDIES OF ALUMINA-GRAPHENE COMPOSITES

K. I. Vishnu Vandana[1*], K.N.S. Suman[2]

[1]Department of Mechanical Engineering, P.V.P.Siddhartha Institute of Technology, Kanuru, Vijayawada, AP, India
[2]Department of Mechanical Engineering, Andhra University, Vishakhapatnam, AP, India

Abstract. In this work, a novel microwave sintering technique is employed to fabricate the Alumina (Al_2O_3)-based composites after reinforcing with graphene particles at different wt% ranging from 0.15 wt% to 0.65 wt% with an interval of 0.1. Attempts are made to identify the effect of sintering temperature on the density of resultant ceramic composite. Once the composites are prepared, the microstructural and mechanical properties (tensile strength and young's modulus) of the samples are studied using scanning electron microscope and universal testing machine, respectively. The scanning electron microscopy (SEM) images of the tensile sample are examined before and after the tensile test to analyse the effect of graphene reinforcement on the alumina ceramic matrix. The Young's modulus of graphene reinforced alumina matrix composites further estimated by using Micromechanics approach and Finite element method. It is interesting to note that a considerable increase in the mechanical properties of the prepared composites is observed with the reinforcement of graphene when compared with monolithic alumina samples prepared under the same experimental conditions.

Keywords: *Alumina (Al_2O_3), Graphene, Tensile strength, Young's modulus, Microstructure.*

Corresponding Author: *K.I. Vishnu Vandana, Assistant Professor, Department of Mechanical Engineering, P.V.P.Siddhartha Institute of Technology, Kanuru, Vijayawada, AP, India, e-mail: kodeyvandana@gmail.com*

Received: *7 October 2021;* ***Accepted:*** *19 November 2021;* ***Published:*** *7 December 2021.*

1. Introduction

Ceramic materials are the most versatile branch of materials. Many strategies have been explored and many authors worked to improve the structure and brittleness of ceramics especially alumina to extend the applications from conventional industry to advanced engineering industry (Kazemzadeh *et al.*, 2009; Jiang *et al.*, 2021; Mudra *et al.*, 2021) . Even much attention on the preparation of alumina composites could not satisfy the requirements of modern engineering needs. Ceramic nano composites, which are made through the reinforcement of appropriate second phase fibers or nano particles, are exhibiting improved functional and mechanical performance compared to pure alumina. Several fillers, such as pumpkin seed husks, titanium carbide (TiC), silicon nitride (Si_4N_3), silicon carbide (SiC) have been used to reinforce ceramics (Sverguzova *et al.*, 2021; Chen *et al.*, 2015; Ohji *et al.*, 1998; Parchovianský *et al.*, 2014). The innovation of carbon nanotubes (CNT) by Iijima (Ma *et al.*, 2010) allowed the enhancement of mechanical and functional properties of alumina. Later, several attempts have been done to prepare alumina matrix composites reinforced with CNTs (Ma *et al.*, 2010; Zhao *et al.*, 2011), which led to the improvement of alumina properties. Even the

optimum strength and elasticity of CNTs could not fully fulfil the required properties of alumina ceramics due to agglomerating natures of CNTs at higher loading level in resultant composite (Sharma *et al.,* 2019). Meanwhile, graphene, a novel reinforcing material awakened the thoughts of several authors in devising the new alumina ceramic nano composite (Markandan *et al.,* 2017). The remarkable elasticity, mechanical strength and unique characteristics predicted for graphene, if reinforced and sintered properly in the matrix, converts alumina in to a stronger and tougher material (Liu *et al.,* 2014). Few studies have focused on the reinforcement of graphene in the alumina matrix and reported enhanced properties of obtained composite (Porwal *et al.,* 2013).

To get desired functional and mechanical properties of alumina-graphene nano composites, a better sintering process and homogenous distribution of graphene in the alumina matrix are vital. In this regard, many authors adopted SPS and HP sintering methods to prepare the alumina ceramic composites (Santanach *et al.,* 2011; Hansson *et al.,* 1993). Many studies have reported improved mechanical and thermal properties of alumina graphene composite when processed using spark plasma sintering and hot pressing (HP) (Bisht *et al.,* 2017; Rutkowski *et al.,* 2015). On the other hand, when the composite ceramics are sintered by hot pressing (HP) or spark plasma sintering (SPS), composite usually experience very high sintering temperature for long period of time to get full densification and may consume high energy respectively. These sintering conditions generally will result unusual grain growth and non-homogeneous microstructure in the resulting composite, limiting the improvement in mechanical properties and economic viability of sintered composites (Cheng *et al.,* 2017). Hence, it is essential to choose an innovative sintering technology to obtain the full benefits of densification. At the same time, the process of sintering should facilitate low grain growth in the resulting composite.

Microwave sintering has some unique characteristics when compared to conventional sintering. In conventional sintering, entire furnace section is heated through radiative heat transfer by using interactive electromagnetic waves, as a result, this process increases the consumption of energy. But the use of microwave sintering significantly reduces the consumption of energy, especially in high temperature processes, as it doesn't heat the components of furnace by its process. Still, the advantages of using microwave sintering in high-temperature courses are not only limited to savings of energy, but also in improving the sintered product quality (Menezes *et al.,* 2012; Cheng *et al.,* 2017). Very limited literature is available on the investigation of microwave sintered alumina graphene composites. Hence in the present work, novel microwave sintering is adopted to prepare alumina graphene composites.

Mechanical properties like tensile strength and young's modulus of material are very crucial in deciding the material's performance during it's functioning and applications in different areas. So, several researchers tried to improve the modulus strength of alumina by reinforcing it with different materials like Zirconia, CNTs, and Graphene oxide. Tuan et al. (2002), prepared a composite using pressure less sintering by incorporating particles of t-phase and m-phase zirconia in to the alumina matrix and reported the improved strength and modulus values of the obtained alumina composite. Kim et al. (2009) also prepared alumina composite by incorporating carbon nano tubes in to alumina matrix and reported improved modulus and strength of resulting composite. But there is very limited research and study on effect of graphene on tensile strength and modulus of alumina composite prepared by microwave sintering process. Hence in the present work, tensile strength and young's modulus values of microwave sintered alumina

graphene composite samples were obtained by carrying out tensile tests. Effect of different weight %s of graphene on the mechanical properties of the resulting alumina ceramic composite was also studied. Microstructures of samples are analysed using SEM images before and after tensile test and are reported. Substantial improvement observed in the prepared composite is paving the way for further research on applications of alumina graphene composites in various fields.

2. Methodology

2.1 Composite Material Preparation and Densification

Commercial Alumina ceramic powder with particle size of 300 nm is used as the base material in the preparation of the present composite. Graphene powder (from AD-NANO TECHNOLOGIES Bangalore) with a nominal size of around 3-8 nm was reinforced in to alumina matrix basing on wt% at an interval of 0.1 ranging from 0.15 to 0.65 wt% to prepare the composite ceramic material. In the ethanol medium, the powders are well mixed and processed using a ball mill for four hours to ensure uniform mixture. Green alumina-Graphene composite samples are prepared in the required shape and size using a hydraulic press. To prevent oxidation of pressed samples, they were placed in crucibles filled with SiC powder and were sintered in microwave furnace. Sintering was done at different temperatures ranging from 1300^0C, 1400^0C, and 1500^0C holding the samples for 30 minutes in each case. Archimedes' principle was employed to measure density of the prepared samples Table. 1 represents the compositions and corresponding densities of prepared ceramic samples.

Table. 1. Composition and corresponding Densities of prepared composite samples

Composition of Graphene in Alumina wt%	Sample	Sintering Conditions	Density (g/cc)	Theoretical Density (%)
A:0.15	Alumina-Graphene(0.15 wt%)	1300°C/30Min	3.23	81.41
		1400^0C/30Min	3.5	88.22
		1500°C/30Min	3.85	96.95
B:0.25	Alumina-Graphene(0.25 wt%)	1300°C/30Min	3.31	83.46
		1400^0C/30Min	3.62	91.28
		1500°C/30Min	3.89	98.2
C:0.35	Alumina-Graphene(0.35 wt%)	1300°C/30Min	3.51	88.58
		1400^0C/30Min	3.78	95.36
		1500°C/30Min	3.96	99.90
D:0.45	Alumina-Graphene(0.45 wt%)	1300°C/30Min	3.41	86.06
		1400^0C/30Min	3.55	89.60
		1500°C/30Min	3.89	98
E:0.55	Alumina-Graphene(0.55 wt%)	1300°C/30Min	3.31	83.58
		1400^0C/30Min	3.52	88.88
		1500°C/30Min	3.85	97.12
F:0.65	Alumina-Graphene(0.65 wt%)	1300°C/30Min	3.21	81.09
		1400^0C/30Min	3.53	89.17
		1500°C/30Min	3.81	96.11

Fig. 1 indicates theoretical density of prepared composite samples at different sintered temperatures. From Fig. 1 it is very clear that maximum density for all alumina-graphene

composites samples was obtained at 1500^0C sintered temperature. And from Fig. 1, it is also evident that alumina-graphene composite containing 0.35 wt% and 0.45 wt% samples got highest relative density.

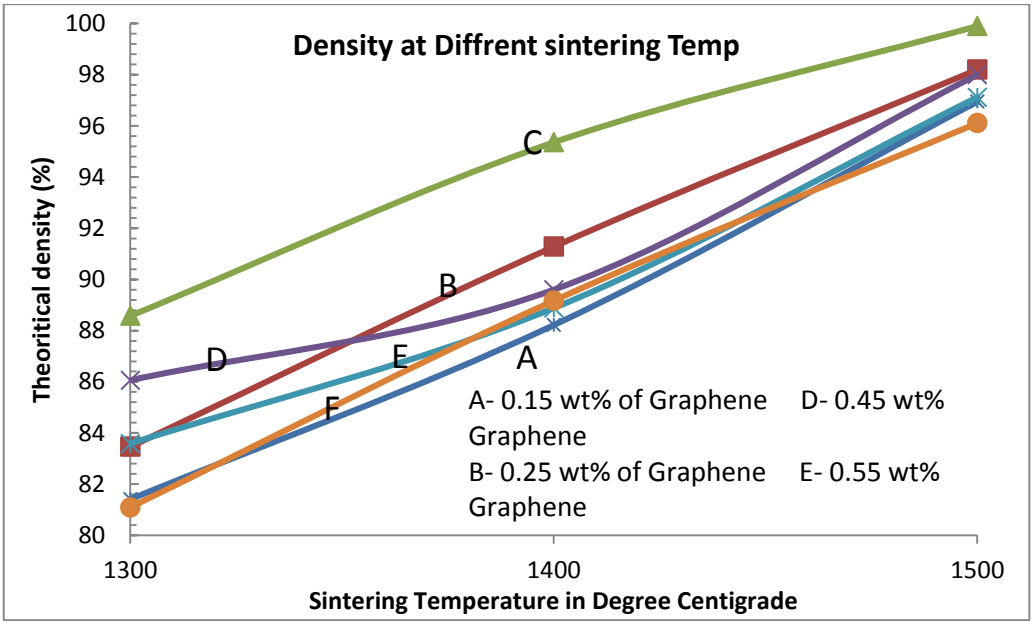

Fig 1. Density of prepared Alumina-Graphene composites at different sintering temperatures

Basing on this data, for further experimentation remaining all samples are sintered at 1500^0C temperature only. Monolithic alumina samples are also prepared under similar conditions i.e. without adding graphene.

2.2 Tensile Test

Samples are prepared according to standard required to perform tensile test. Then tensile strength of prepared alumina graphene composite samples was tested using a computer-controlled Nano 25 KN Universal Testing Machine (UTM). A controlling speed of 0.4 mm/min was employed during testing. Ultimate tensile strength and elastic modulus of samples are obtained from the load deflection curve. Each test was performed on two samples and results are averaged. The morphology of each specimen is analysed using SEM images before and after the tensile test.

3. Results and Discussions

3.1 Morphology

Fig. 2 shows the dispersion of different wt%s of reinforced graphene nano particles in the alumina matrix. From Fig. 3(a) to 3(d), it is very clear that graphene particles are well dispersed and placed at grain boundary of the alumina at 0.15 wt% of graphene and it continued up to 0.45 wt% of graphene composite samples. The embedded graphene particle around the grain boundaries of alumina reduces the growth of grain boundaries and further refines the microstructure. When abnormal grain growth is restricted, automatically the size of the grains reduces and increases the surface to volume ratio. The increased surface to volume ratio increases the grain boundary, which restricts the dislocations in the structure. The homogenous dispersion of graphene in the alumina

matrix seems to be responsible for achieving good density by reducing grain growth in the prepared composite samples. The unique homogeneous heating process of microwave sintering might facilitate graphene particles to disperse uniformly in the alumina matrix up to definite wt% of graphene. But the graphene particles are seemed to overlap with each other in composite samples containing 0.55 wt% of graphene and 0.65 wt% of graphene which indicates agglomeration tendency of graphene particles and was shown in Fig. 2(e) and Fig. 2(f). The accumulation can be attributed to increased concentration of graphene particles in the alumina matrix. This overlapping of graphene generally makes the alumina grain boundaries weak and contributes to the grain growth thus reducing the compactness and density of the composite. And this can also be observed through the values of relative density of different composite samples from Table. 1. Samples with 0.35 wt% and 0.45 wt% of graphene are exhibiting high relative density and remaining composite samples are exhibiting low relative density.

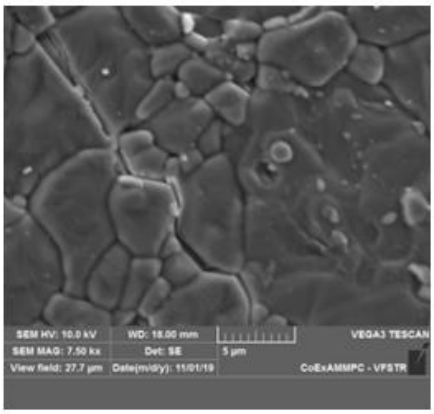

(a): Composite with 0.15wt% of Graphene

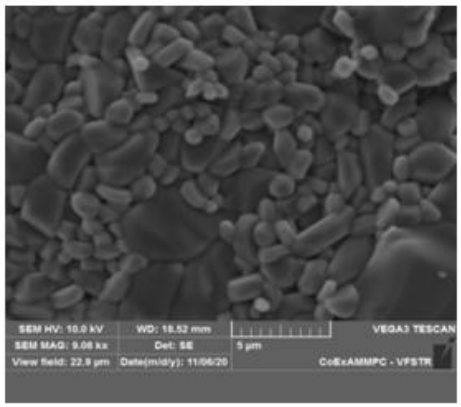

(b): Composite with 0.25wt% of Graphene

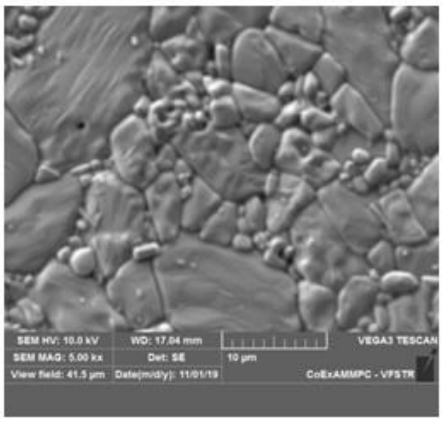

(c): Composite with 0.35wt% of Graphene

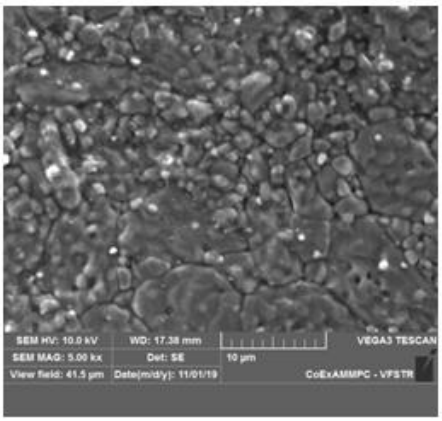

(d): Composite with 0.45wt% of Graphene

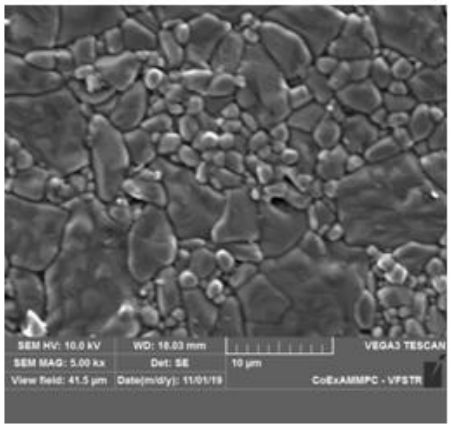

(e) : Composite with 0.55wt% of Graphene

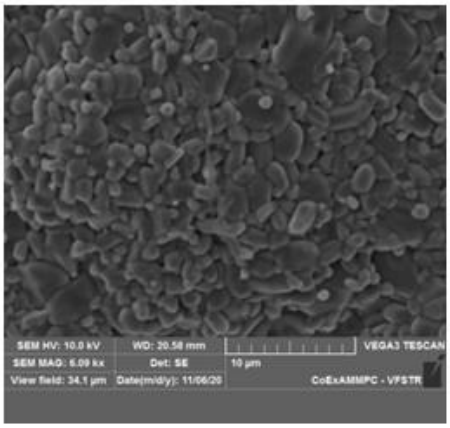

(f): Composite with 0.65wt% of Graphene

Fig. 2. SEM images of dispersion of reinforced graphene (different wt%s) in the alumina matrix

3.2 Tensile Properties: Table 2 represents values of ultimate tensile strength and young's modulus of prepared alumina graphene nano composites.

Table. 2. Tensile strength and Young's modulus of prepared Alumina-graphene composite

Composite	Ultimate Tensile Strength (MPa)	Young's Modulus (GPa)
Monolithic Alumina	146.77	380
Al-G(0.15 wt%)	150.61	385
Al-G(0.25 wt%)	158.52	395
Al-G(0.35 wt%)	169.33	398
Al-G(0.45 wt%)	172.87	395
Al-G(0.55 wt%)	150.21	380
Al-G(0.65 wt%)	146.66	376

Fig. 3 and Fig. 4 indicate the response of Ultimate tensile strength and Young's modulus parameter values of prepared composite samples for different wt% of graphene reinforced in the alumina matrix. When compared with tensile strength of monolithic alumina samples, tensile strength of the prepared composite samples was increased up to 0.45 wt% of graphene reinforcement. The % of increase in the tensile strength was 2.61%, 8.00%, 15.37% and 17.78% for 0.15 wt%, 0.25 wt%, 0.35 wt% and 0.45 wt% of graphene reinforced composite samples respectively when compared with monolithic alumina samples. With the homogeneous and uniform dispersion of graphene in the ceramic matrix, abnormal grain growth was restricted and will leave the structure with normal sized grains. The small and normal sized grains automatically increase the strength of the composite. Later tensile strength was decreased from 0.55 wt% of graphene reinforced ceramic composite samples when compared with 0.45 wt% of graphene reinforced ceramic composite samples. The tensile strength value for 0.65 wt% of graphene reinforced ceramic composite sample was same as monolithic alumina sample tensile strength.

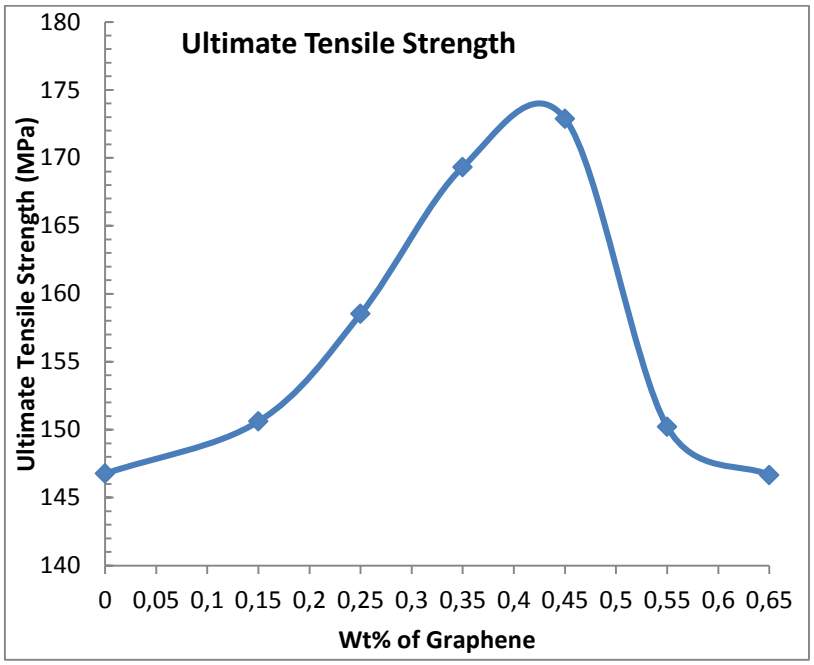

Fig. 3. Ultimate Tensile Strength of Composite samples at different wt% of grapheme

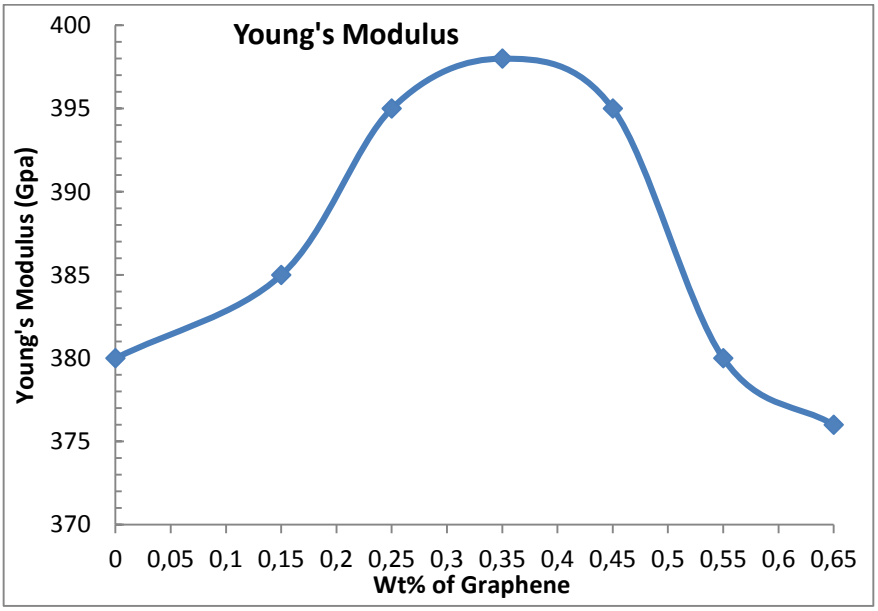

Figure 4. Young's Modulus of Composite samples at different wt% of graphene

From Fig. 4 it is prominent that, the Young's modulus of the prepared composite samples is increased up to 0.45 wt% of graphene reinforced alumina composite samples and was same at 0.55 wt% graphene reinforced alumina composite samples, when compared with young's modulus of monolithic alumina samples. The % of increase in young's modulus was 1.31%, 3.94%, 4.73%, 3.94% for 0.15 wt%, 0.25 wt% 0.35 wt%, 0.45 wt% of graphene reinforced alumina composite samples respectively when compared with monolithic alumina samples. The young's modulus value of 0.55 wt%

graphene reinforced composite sample was same as young's modulus value of monolithic alumina sample. But the young's modulus of 0.65 wt% of graphene reinforced composite samples was reduced when compared with young's modulus value of monolithic alumina samples. The sudden decrease in the values of tensile strength and young's modulus from 0.55 wt% of graphene reinforced composite samples may be due to the increased loading of graphene wt%. The increased loading of graphene particles in alumina matrix leads to formation of more number of graphene inter linked flake sites. These interlink graphene sites works as catalysts and provoke the microstructural defects which lead to reduced density of the samples. This can also be observed from Table 1. The reduced density might directly influence negatively the toughness and modulus values of composites samples.

3.3 Fractographical Studies

Fig. 5(a) to 5(g) are the fractured surface SEM images of prepared composite samples after performing tensile load test. The detailed pattern of fractures behaviour in the composite sample surfaces can be observed from the SEM images. The appearance of more roughness on the fractured surface suggests a possible crack deflection mechanism generally in case of tensile materials (Hansson *et al.,* 1993). Deflection of the induced crack, when met with an obstacle, gives the toughening effect. During this process to avoid the obstacles, crack tips tilt and twist for elongated crack lengths. This results in small dimples or shallowness on the fractured surface which appears like rougher surface. On the other side, a smooth and essentially featureless fractured surface indicates brittleness in the tested sample. Fig. 5(a) shows the typical fractured surface of the monolithic alumina sample. Most of the surface is smooth and essentially featureless, indicating the brittleness of alumina ceramic. From Fig. 5(b) to 5(e), a small rate of increase in the roughness of fractured surfaces can be observed with the presence of dimples on the surface. The dimples observed clearly in Fig. 5(d) and Fig. 5(e) are the indication of possible crack deflections and improved toughness in the composite. As ductility and toughness were strongly dependent on second phase material, the increased toughness in the composite can be attributed to superior qualities of graphene as well as uniform dispersion of graphene particles at the grain boundaries. As graphene reinforcement percentage is increasing in the base matrix, the toughening effect seems to be increasing in the resultant composite sample. And this effect seems to be elevated in the alumina composite sample containing 0.35 wt% of graphene and 0.45 wt% of graphene. But from Fig. 7(f) to Fig. 7(g), the fractured surfaces are observed to be having finished surfaces with very few numbers of dimples and shallow marks indicating the reduced toughness in the composite. Fig. 7(g) the fractured surface with 0.65 wt% of graphene seems to be smooth indicating further reduced toughness. The increased loading of graphene particles in the composite sample was observed to increase attachment of graphene particles in Fig. 2(d) and Fig. 2(e). The attachment or agglomeration of graphene particles leads to weak bonding interaction with the alumina particles which reduces the interfacial adhesion between the alumina matrix and reinforced graphene thereby reducing the toughness of resulting composite. Fractured surfaces of composite samples with reduced toughness will exhibit more finished surface as shown in Fig. 5(f) and Fig. 5(g) with relatively less number of dimples, when compared with Fig. 5(d) and Fig. 5(e).

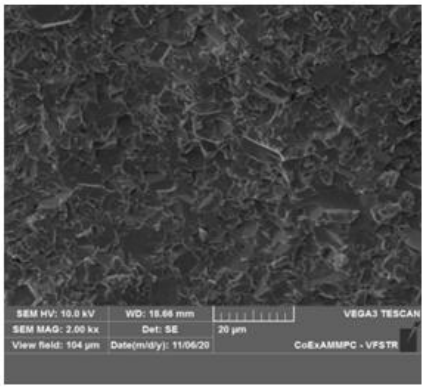

(a)Monolithic Alumina sample

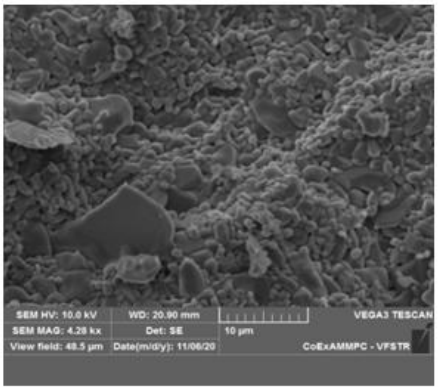

(b): Composite with 0.15wt% of Graphene

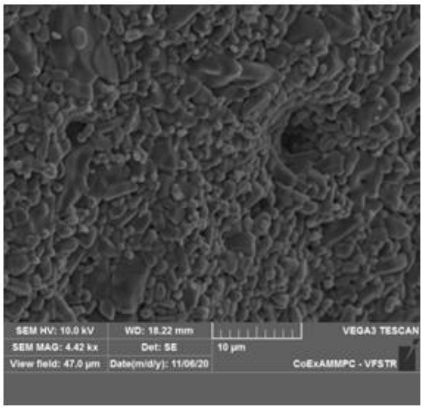

(c): Composite with 0.25wt% of Graphene

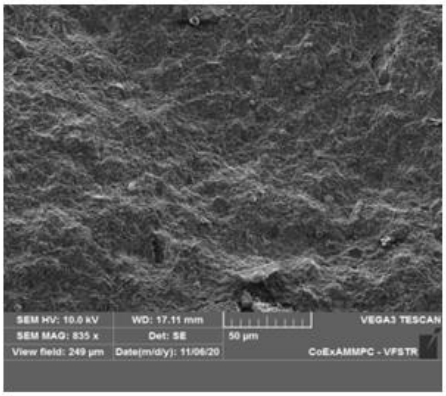

(d): Composite with 0.35wt% of Graphene

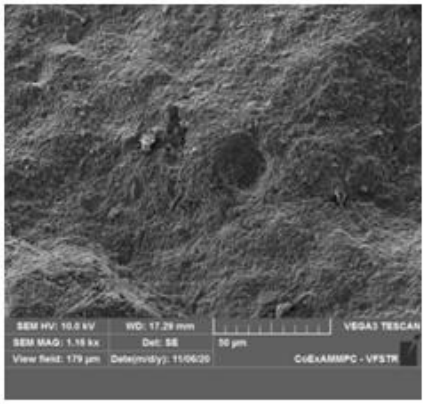

(e) : Composite with 0.45wt% of Graphene

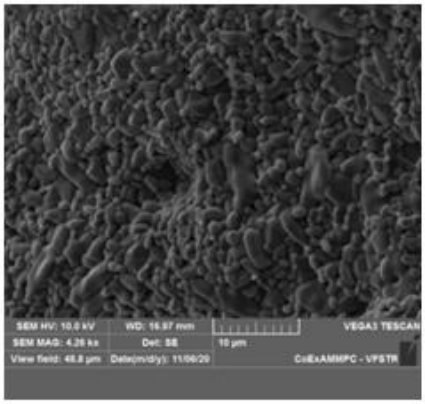

(f): Composite with 0.55wt% of Graphene

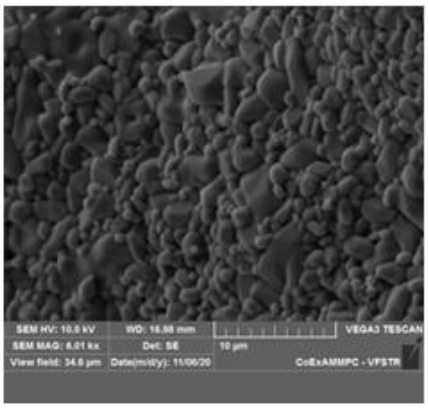

(g): Composite with 0.65wt% of Graphene

Fig. 5. SEM images of fractured Alumina-Graphene samples after Tensile Test

3.4 Micromechanical Studies

The Micromechanics studies carried by assuming uniform distribution of graphene in the alumina matrix and the graphene powder is idealized as a spherical particle. The perfect bonding is assumed between the particles and the matrix material. The spherical particles are can be idealized for the graphene powder and theses particles can be distributed in the alumina matrix as presented below in Fig. 6.

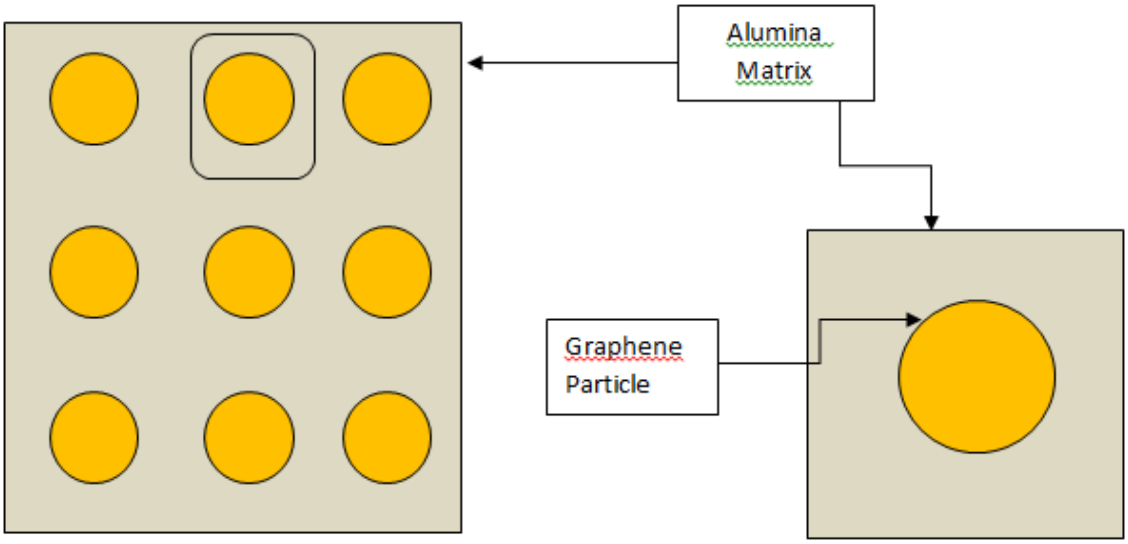

Fig. 6. Idealization of graphene particle in alumina matrix and one unit cell

Considering the advantages of symmetry of geometrical model, loading and boundary conditions, one eighth portion of the graphene particle is considered in the final analysis. After considering the advantage of the symmetry, the model is treated for the analysis.

3.4.1 Element Type: Solid 20 node 186 element was selected for both particle and matrix materials discretization. Solid 186 element is defined by 20 nodes and each node have 6 degrees of freedom. The dimensions of the FE model are calculated based on

radius of the particle and volume fraction of the graphene powder Fig. 7. The graphene powder diameter and elastic properties are collected from published literature. The Young's modulus of the graphene reinforcement is 1 TPa and Poisson's ratio is 0.3. The alumina Young's modulus is 380 GPa and Poisson's ratio is 0.35. Using, roller supports, multipoint constrains, and applying the Hook's law, the modulus, Poisson's ratio was determined.

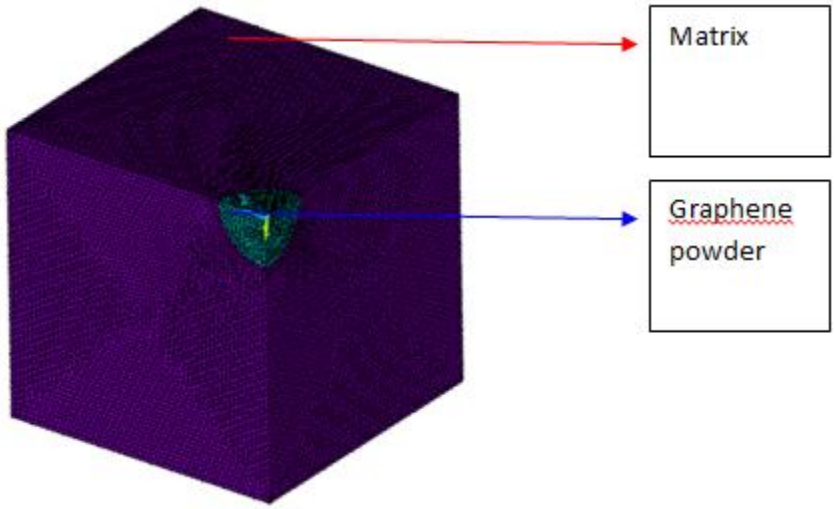

Fig. 7. Finite Element model at 0.28% volume fraction

Loading and Boundary conditions: Due to the symmetry of the Finite element model, the following symmetric boundary conditions are used. The nodes corresponding to x=0 area are resiticted to move in X-direction and similarly the nodes corresponding t0 Y=0, Z=0 are restricted in Y and Z- directions respectively. Multipoint constains are also applied on the nodes corresponding to positive X,Y and Z directions respectively. Uniform tensile load of 1 Mpa is applied on the positive Z-face. Using the Hook's law, the Young's modulus is identified from FE models (Phani Prasanthi *et al.*, 2019).

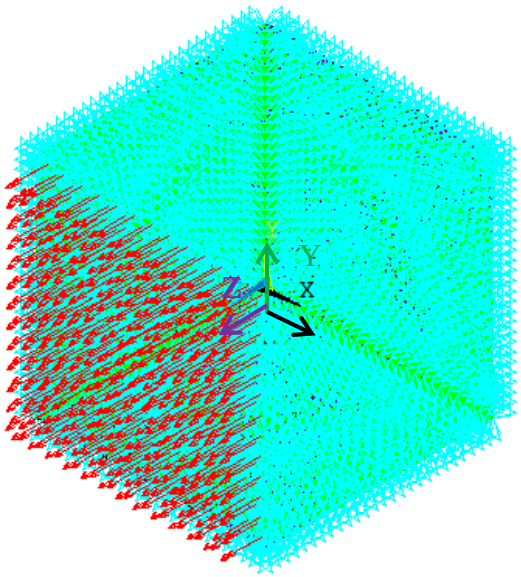

Figure 8. Loading and boundary condition on the FE model

The properties are estimated from FE models and the results are presented in Table. 3.

Table 3. Young's Modulus values of composite From FE model

Volume Fraction of Graphene powder	Young's modulus from FE models [GPa]	From Experiments GPa	Percentage of error (%)
0.28	388	385	0.77
0.47	401	395	1.51
0.66	403	398	1.25
0.85	400	395	1.26
1.03	386	380	1.57
1.22	379	376	0.79

The Finite element procedures for the evaluation of the properties and validation of Finite models are presented in the present study are shown as in Fig. 9 and Fig. 10.

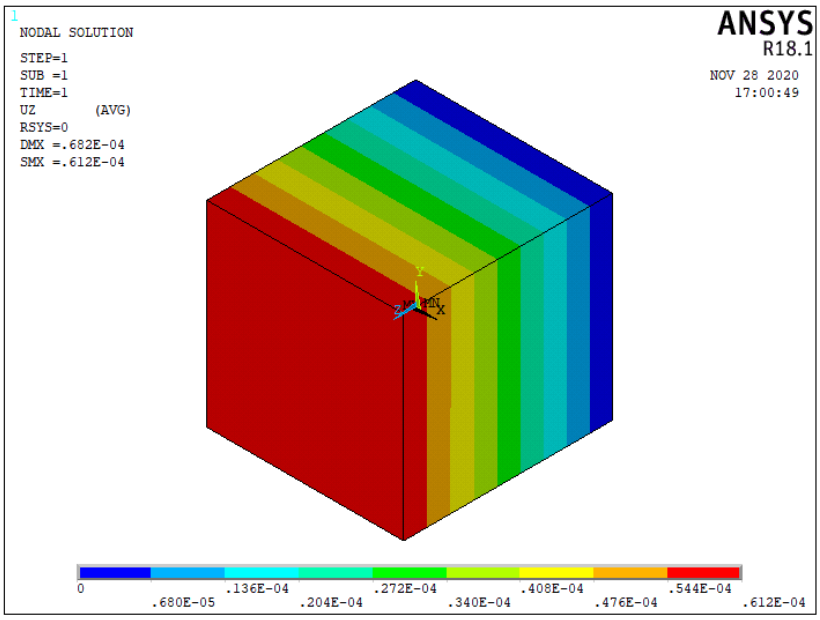

Figure 9. Deformation in loading direction

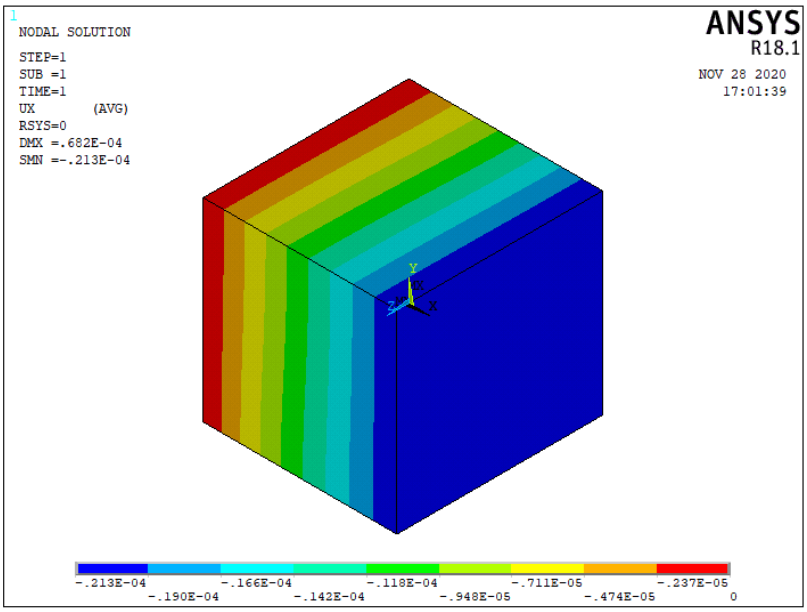

Figure 10. Deformation in transverse direction

4. Conclusion

1. Alumina – Graphene composite samples with varying wt% of graphene, were prepared using novel microwave sintering technique.
2. Nearly fully dense (> 99%) alumina –graphene composite was obtained at 0.35 wt% of reinforcement of graphene. Composite samples with good (relative density 98%) density were obtained at 0.35 wt% and 0.45 wt% of graphene reinforcement.
3. Well dispersion and reduced grain growth are observed in the obtained composite samples especially with 0.35 wt% and 0.45 wt% of reinforcement of graphene. Local overlapping of graphene particles was observed with the increasing quantity of graphene reinforcement i.e more than 0.45 wt%.
4. SEM analysis and tensile test revealed the improved toughening effect of alumina-graphene composite samples when compared with monolithic alumina and are seems to be elevated at 0.35 wt% and 0.45 wt% of graphene reinforcement. This indicates enhanced stress bearing capabilities of the produced alumina-graphene composite.
5. When compared with Young's modulus values of monolithic alumina, values of composite also increased with increased reinforcement of graphene and are observed to be elevated up to 0.45 wt% of reinforcement of graphene.
6. FE models are also revealing that prepared composite samples with 0.35 wt% and 0.45 wt% reinforced graphene are exhibiting improved properties when compared with monolithic alumina.
7. The present work finally concludes that graphene reinforcement in alumina is exhibiting potential improvement in properties of resulting alumina-graphene composite. Alumina graphene composite samples with 0.35 wt% and 0.45 wt% reinforced graphene are exhibiting improved mechanical properties when compared with monolithic alumina.

References

Bisht, A., Srivastava, M., Kumar, R.M., Lahiri, I., & Lahiri, D. (2017). Strengthening mechanism in graphene nanoplatelets reinforced aluminum composite fabricated through spark plasma sintering. *Materials Science and Engineering: A*, *695*, 20-28.

Chen, F., Yang, S., Wu, J., Galaviz Perez, J. A., Shen, Q., Schoenung, J. M., ... & Zhang, L. (2015). Spark plasma sintering and densification mechanisms of conductive ceramics under coupled thermal/electric fields. *Journal of the American Ceramic Society*, *98*(3), 732-740.

Cheng, Y., Zhang, Y., Wan, T., Yin, Z., & Wang, J. (2017). Mechanical properties and toughening mechanisms of graphene platelets reinforced Al2O3/TiC composite ceramic tool materials by microwave sintering. *Materials Science and Engineering: A*, *680*, 190-196.

Hansson, T., Warren, R., & Wasén, J. (1993). Fracture Toughness Anisotropy and Toughening Mechanisms of a Hot-Pressed Alumina Reinforced with Silicon Carbide Whiskers. *Journal of the American Ceramic Society*, *76*(4), 841-848.

Iijima, S. (1991). Helical microtubules of graphitic carbon. *Nature*, *354*(6348), 56-58.

Jiang, R., Sun, X., Liu, H., Liu, Y., & Mao, W. (2021). Microstructure and mechanical properties improvement of the Nextel™ 610 fiber reinforced alumina composite. *Journal of the European Ceramic Society*, *41*(10), 5394-5399.

Kazemzadeh, A., Rahimipour, M.R., Salahi, E., Yazdani, R., Razavi Tousi, S.S., & Razavi, M. (2009). Structural evolution of Al-20%(Wt) Al2O3 system during ball milling stages. *International Journal of Engineering*, *22*(2), 169-178.

Kim, S.W., Chung, W.S., Sohn, K.S., Son, C.Y., & Lee, S. (2009). Improvement of flexure strength and fracture toughness in alumina matrix composites reinforced with carbon nanotubes. *Materials Science and Engineering: A*, *517*(1-2), 293-299.

Liu X., Fan Y-C., Li J.-L., Wang L.-J., & Jiang W.(2014). Preparation and Mechanical Properties of Graphene Nanosheet Reinforced Alumina Composites. *Advanced Energy Materials*. DOI: 10.1002/adem.201400231.

Ma, P.C., Siddiqui, N.A., Marom, G., & Kim, J.K. (2010). Dispersion and functionalization of carbon nanotubes for polymer-based nanocomposites: A review. *Composites Part A: Applied Science and Manufacturing*, *41*(10), 1345-1367.

Markandan, K., Chin, J.K., & Tan, M.T. (2017). Recent progress in graphene based ceramic composites: a review. *Journal of Materials Research*, *32*(1), 84-106.

Menezes, R.R., Souto, P.M., & Kiminami, R.H.G.A. (2012). Microwave fast sintering of ceramic materials. *Sintering of Ceramics–New Emerging Techniques*, *1*, 3-26..

Mudra, E., Shepa, I., Hrubovcakova, M., Koribanich, I., Medved, D., Kovalcikova, A., ... & Dusza, J. (2021). Highly wear-resistant alumina/graphene layered and fiber-reinforced composites. *Wear*, *484*, 204026..

Ohji, T., Jeong, Y.K., Choa, Y.H., & Niihara, K. (1998). Strengthening and toughening mechanisms of ceramic nanocomposites. *Journal of the American Ceramic Society*, *81*(6), 1453-1460.

Parchovianský, M., Galusek, D., Michálek, M., Švančárek, P., Kašiarová, M., Dusza, J., & Hnatko, M. (2014). Effect of the volume fraction of SiC on the microstructure and creep behavior of hot pressed Al2O3/SiC composites. *Ceramics International*, *40*(1), 1807-1814.

Phani Prasanthi, K. Sivaji Babu, M. S. R. Niranjan Kumar & A. Eswar Kumar (2021) Analysis of Sisal Fiber Waviness Effect on the Elastic Properties of Natural Composites Using Analytical and Experimental Methods, *Journal of Natural Fibers*, *18*(11), 1675-1688, DOI: 10.1080/15440478.2019.1697987.

Porwal, H., Tatarko, P., Grasso, S., Khaliq, J., Dlouhý, I., & Reece, M. J. (2013). Graphene reinforced alumina nano-composites. *Carbon*, *64*, 359-369.

Rutkowski P., Klimczyk P., Jaworska L., Stobierski L., & Dubiel A. (2015). Thermal properties of pressure sintered alumina–graphene composites, *Journal of Thermal Analysis and Calorimetry*, 122, 105–114.

Santanach, J. G., Weibel, A., Estournès, C., Yang, Q., Laurent, C., & Peigney, A. (2011). Spark plasma sintering of alumina: Study of parameters, formal sintering analysis and hypotheses on the mechanism (s) involved in densification and grain growth. *Acta Materialia*, *59*(4), 1400-1408.

Sharma, N., Syed, A.N., Ray, B.C., Yadav, S., & Biswas, K. (2019). Alumina–MWCNT composites: microstructural characterization and mechanical properties. *Journal of Asian Ceramic Societies*, *7*(1), 1-19.

Sverguzova, S., Miroshnichenko, N., Shaikhiev, I., Sapronova, Z., Fomina, E., Shakurova, N., & Promakhov, V. (2021). Application of Sorbent Waste Material for Porous Ceramics Production. *International Journal of Engineering*, *34*(3), 621-628.

Tuan, W. H., Chen, R. Z., Wang, T. C., Cheng, C. H., & Kuo, P. S. (2002). Mechanical properties of Al2O3/ZrO2 composites. *Journal of the European Ceramic Society*, *22*(16), 2827-2833.

Zhao, J. S., Feng, Y., Chen, N. N., Chen, F. Y., Chen, J., Zhang, X. B., ... & Ouyang, X. P. (2011). Fabrication and Mechanical Properties of Alumina—CNTs Composites. In *Applied Mechanics and Materials* (Vol. 66, pp. 1390-1396). Trans Tech Publications Ltd.